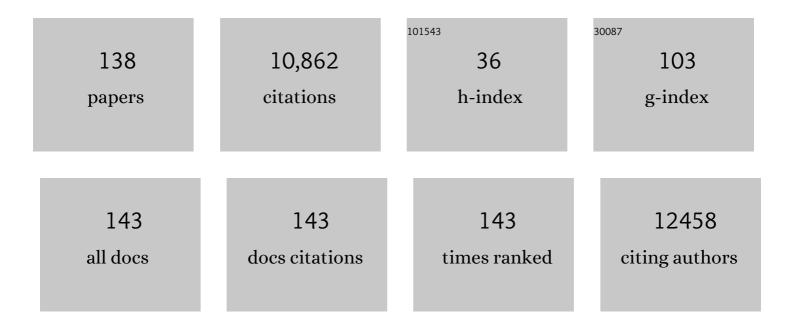
List of Publications by Year in descending order

Source: https://exaly.com/author-pdf/2130911/publications.pdf Version: 2024-02-01



#	Article	IF	CITATIONS
1	Schottky Diode with Asymmetric Metal Contacts on WS ₂ . Advanced Electronic Materials, 2022, 8, 2100941.	5.1	12
2	Super-Nernstian pH Sensor Based on Anomalous Charge Transfer Doping of Defect-Engineered Graphene. Nano Letters, 2021, 21, 34-42.	9.1	29
3	Realization of Waferâ€Scale 1Tâ€MoS ₂ Film for Efficient Hydrogen Evolution Reaction. ChemSusChem, 2021, 14, 1344-1350.	6.8	21
4	A phase-convertible fast ionic conductor with a monolithic plastic crystalline host. Journal of Materials Chemistry A, 2021, 9, 10838-10845.	10.3	3
5	Improved Contact Resistance by a Single Atomic Layer Tunneling Effect in WS 2 /MoTe 2 Heterostructures. Advanced Science, 2021, 8, 2100102.	11.2	11
6	Solution-Processed MoS ₂ Film with Functional Interfaces via Precursor-Assisted Chemical Welding. ACS Applied Materials & Interfaces, 2021, 13, 12221-12229.	8.0	19
7	Graphene/PVDF Composites for Ni-rich Oxide Cathodes toward High-Energy Density Li-ion Batteries. Materials, 2021, 14, 2271.	2.9	7
8	Graphene collage on Ni-rich layered oxide cathodes for advanced lithium-ion batteries. Nature Communications, 2021, 12, 2145.	12.8	54
9	Defect-Free Mechanical Graphene Transfer Using <i>n-</i> Doping Adhesive Gel Buffer. ACS Nano, 2021, 15, 11276-11284.	14.6	14
10	Controlled growth of in-plane graphene/h-BN heterostructure on a single crystal Ge substrate. Applied Surface Science, 2021, 554, 149655.	6.1	11
11	Performance Improvement of Residue-Free Graphene Field-Effect Transistor Using Au-Assisted Transfer Method. Sensors, 2021, 21, 7262.	3.8	3
12	Self-Catalytic Growth of Elementary Semiconductor Nanowires with Controlled Morphology and Crystallographic Orientation. Nano Letters, 2021, 21, 9909-9915.	9.1	2
13	hBN Flake Embedded Al2O3 Thin Film for Flexible Moisture Barrier. Materials, 2021, 14, 7373.	2.9	1
14	Waferâ€Scale and Lowâ€Temperature Growth of 1Tâ€WS ₂ Film for Efficient and Stable Hydrogen Evolution Reaction. Small, 2020, 16, e1905000.	10.0	53
15	Elucidation of the role of lithium iodide as an additive for the <scp>liquidâ€based</scp> synthesis of <scp> Li ₇ P ₂ S ₈ I </scp> solid electrolyte. International Journal of Energy Research, 2020, 44, 11542-11549.	4.5	3
16	Layer-engineered large-area exfoliation of graphene. Science Advances, 2020, 6, .	10.3	81
17	Highly Efficient n-Type Doping of Graphene by Vacuum Annealed Amine-Rich Macromolecules. Materials, 2020, 13, 2166.	2.9	10
18	Twin boundary sliding in single crystalline Cu and Al nanowires. Acta Materialia, 2020, 196, 69-77.	7.9	10

#	Article	IF	CITATIONS
19	Toward Scalable Growth for Single-Crystal Graphene on Polycrystalline Metal Foil. ACS Nano, 2020, 14, 3141-3149.	14.6	26
20	Hydrogen Evolution Reaction: Waferâ€Scale and Lowâ€Temperature Growth of 1Tâ€WS ₂ Film for Efficient and Stable Hydrogen Evolution Reaction (Small 6/2020). Small, 2020, 16, 2070033.	10.0	2
21	Chemical Vapor Deposition: An Ecoâ€Friendly, CMOSâ€Compatible Transfer Process for Largeâ€Scale CVDâ€Graphene (Adv. Mater. Interfaces 13/2019). Advanced Materials Interfaces, 2019, 6, 1970087.	3.7	0
22	Growth of quantum dot coated core-shell anisotropic nanowires for improved thermal and electronic transport. Applied Physics Letters, 2019, 114, 243104.	3.3	6
23	Rational Design of Ultrathin Gas Barrier Layer via Reconstruction of Hexagonal Boron Nitride Nanoflakes to Enhance the Chemical Stability of Proton Exchange Membrane Fuel Cells. Small, 2019, 15, e1903705.	10.0	15
24	An Ecoâ€Friendly, CMOSâ€Compatible Transfer Process for Largeâ€5cale CVDâ€Graphene. Advanced Materials Interfaces, 2019, 6, 1900084.	3.7	15
25	Graphene on Groupâ€IV Elementary Semiconductors: The Direct Growth Approach and Its Applications. Advanced Materials, 2019, 31, e1803469.	21.0	21
26	Atomic-scale Investigation of Interface Between Graphene Monolayer and Ge(110). Journal of the Korean Physical Society, 2019, 74, 241-244.	0.7	1
27	Methane-Mediated Vapor Transport Growth of Monolayer WSe2 Crystals. Nanomaterials, 2019, 9, 1642.	4.1	1
28	Morphology of Ti on Monolayer Nanocrystalline Graphene and Its Unexpectedly Low Hydrogen Adsorption. Journal of Physical Chemistry C, 2019, 123, 1572-1578.	3.1	6
29	Millimeter-Scale Growth of Single-Oriented Graphene on a Palladium Silicide Amorphous Film. ACS Nano, 2019, 13, 1127-1135.	14.6	1
30	Low-temperature wafer-scale growth of MoS2-graphene heterostructures. Applied Surface Science, 2019, 470, 129-134.	6.1	44
31	Unraveling the Factors Affecting the Electrochemical Performance of MoS ₂ –Carbon Composite Catalysts for Hydrogen Evolution Reaction: Surface Defect and Electrical Resistance of Carbon Supports. ACS Applied Materials & Interfaces, 2019, 11, 5037-5045.	8.0	20
32	Amorphous germanium oxide nanobubbles for lithium-ion battery anode. Materials Research Bulletin, 2019, 110, 24-31.	5.2	21
33	2D Doping Layer for Flexible Transparent Conducting Graphene Electrodes with Low Sheet Resistance and High Stability. Advanced Electronic Materials, 2018, 4, 1700622.	5.1	17
34	One-pot size-controlled growth of graphene-encapsulated germanium nanocrystals. Applied Surface Science, 2018, 440, 553-559.	6.1	2
35	Selectivity of Threefold Symmetry in Epitaxial Alignment of Liquid Crystal Molecules on Macroscale Singleâ€Crystal Graphene. Advanced Materials, 2018, 30, e1802441.	21.0	17
36	Deformation twinning of ultrahigh strength aluminum nanowire. Acta Materialia, 2018, 160, 14-21.	7.9	30

#	Article	IF	CITATIONS
37	Controlling electric potential to inhibit solid-electrolyte interphase formation on nanowire anodes for ultrafast lithium-ion batteries. Nature Communications, 2018, 9, 3461.	12.8	27
38	Realization of continuous Zachariasen carbon monolayer. Science Advances, 2017, 3, e1601821.	10.3	46
39	Loose-fit graphitic encapsulation of silicon nanowire for one-dimensional Si anode design. Journal of Materials Science and Technology, 2017, 33, 1120-1127.	10.7	8
40	CMOS-compatible catalytic growth of graphene on a silicon dioxide substrate. Applied Physics Letters, 2016, 109, .	3.3	14
41	A pseudo-capacitive chalcogenide-based electrode with dense 1-dimensional nanoarrays for enhanced energy density in asymmetric supercapacitors. Journal of Materials Chemistry A, 2016, 4, 10084-10090.	10.3	55
42	Large reduction in thermal conductivity for SiGe alloy nanowire wrapped with a Ge nanoparticle-embedded SiO ₂ shell. Nanotechnology, 2016, 27, 305703.	2.6	5
43	Ultralow power complementary inverter circuits using axially doped p- and n-channel Si nanowire field effect transistors. Nanoscale, 2016, 8, 12022-12028.	5.6	6
44	Catalytic etching of monolayer graphene at low temperature via carbon oxidation. Physical Chemistry Chemical Physics, 2016, 18, 101-109.	2.8	16
45	Thermoelectric Properties of Nanowires with a Graphitic Shell. ChemSusChem, 2015, 8, 2372-2377.	6.8	3
46	Ultralow-power non-volatile memory cells based on P(VDF-TrFE) ferroelectric-gate CMOS silicon nanowire channel field-effect transistors. Nanoscale, 2015, 7, 11660-11666.	5.6	14
47	Epitaxial Growth of a Single-Crystal Hybridized Boron Nitride and Graphene Layer on a Wide-Band Gap Semiconductor. Journal of the American Chemical Society, 2015, 137, 6897-6905.	13.7	55
48	Ultrastable-Stealth Large Gold Nanoparticles with DNA Directed Biological Functionality. Langmuir, 2015, 31, 13773-13782.	3.5	29
49	Water-induced room-temperature transformation of straight Ge/Si core/shell nanowires into circular silica nanotubes. CrystEngComm, 2015, 17, 6142-6148.	2.6	0
50	Low-Programmable-Voltage Nonvolatile Memory Devices Based on Omega-shaped Gate Organic Ferroelectric P(VDF-TrFE) Field Effect Transistors Using p-type Silicon Nanowire Channels. Nano-Micro Letters, 2015, 7, 35-41.	27.0	20
51	Carbon out-diffusion mechanism for direct graphene growth on a silicon surface. Acta Materialia, 2015, 96, 18-23.	7.9	8
52	Wafer-Scale Growth of Single-Crystal Monolayer Graphene on Reusable Hydrogen-Terminated Germanium. Science, 2014, 344, 286-289.	12.6	831
53	Core–shell Si _{1â^'x} Ge _x nanowires with controlled structural defects for phonon scattering enhancement. Journal of Materials Chemistry A, 2014, 2, 12153-12157.	10.3	9
54	High performance Si nanowire field-effect-transistors based on a CMOS inverter with tunable threshold voltage. Nanoscale, 2014, 6, 5479.	5.6	8

#	Article	IF	CITATIONS
55	Tunable threshold voltage of an n-type Si nanowire ferroelectric-gate field effect transistor for high-performance nonvolatile memory applications. Nanotechnology, 2014, 25, 205201.	2.6	13
56	Reliability Enhancement of Germanium Nanowires Using Graphene as a Protective Layer: Aspect of Thermal Stability. ACS Applied Materials & Interfaces, 2014, 6, 5069-5074.	8.0	9
57	Physicsâ€based modeling and microwave characterization of graphene coâ€planar waveguides. Physica Status Solidi - Rapid Research Letters, 2014, 8, 617-620.	2.4	2
58	Diameter-Controlled and Surface-Modified Sb2Se3 Nanowires and Their Photodetector Performance. Scientific Reports, 2014, 4, 6714.	3.3	59
59	A facile route to Si nanowire gate-all-around field effect transistors with a steep subthreshold slope. Nanoscale, 2013, 5, 8968.	5.6	11
60	Single inorganic-organic hybrid photovoltaic nanorod. Applied Physics Letters, 2013, 103, 143101.	3.3	5
61	Graphene shell on silica nanowires toward a nanostructured electrode with controlled morphology. Applied Physics Letters, 2013, 103, .	3.3	5
62	Entangled Germanium Nanowires and Graphite Nanofibers for the Anode of Lithium-Ion Batteries. Journal of the Electrochemical Society, 2013, 160, A112-A116.	2.9	31
63	Tunable bandgap of a single layer graphene doped by the manganese oxide using the electrochemical doping. Applied Physics Letters, 2013, 102, 032106.	3.3	17
64	Synthesized Aluminum Nanowires for Future Interconnects [Nanopackaging]. IEEE Nanotechnology Magazine, 2012, 6, 24-26.	1.3	0
65	Control of selective and catalyst-free growth of Sb2Te3 and Te nanowires from sputter-deposited Al-Sb-Te thin films. CrystEngComm, 2012, 14, 4255.	2.6	7
66	The influence of phonon scatterings on the thermal conductivity of SiGe nanowires. Applied Physics Letters, 2012, 101, 043114.	3.3	37
67	Morphology Control of Self-Catalyzed Germanium Nanostructures with Graphitic Carbon Shell. Journal of Nanoscience and Nanotechnology, 2012, 12, 4103-4107.	0.9	0
68	Silicon Embedded Nanoporous Carbon Composite for the Anode of Li Ion Batteries. Journal of the Electrochemical Society, 2012, 159, A1273-A1277.	2.9	12
69	Metastable Ge _{1–<i>x</i>} C _{<i>x</i>} Alloy Nanowires. ACS Applied Materials & Interfaces, 2012, 4, 805-810.	8.0	3
70	Large Thermoelectric Figure-of-Merits from SiGe Nanowires by Simultaneously Measuring Electrical and Thermal Transport Properties. Nano Letters, 2012, 12, 2918-2923.	9.1	181
71	Control of Lateral Dimension in Metal-Catalyzed Germanium Nanowire Growth: Usage of Carbon Sheath. Nano Letters, 2012, 12, 4007-4012.	9.1	12
72	Gate-dependent photoconductivity of single layer graphene grafted with metalloporphyrin molecules. Applied Physics Letters, 2012, 100, .	3.3	6

#	Article	IF	CITATIONS
73	Seed-free electrochemical growth of ZnO nanotube arrays on single-layer graphene. Materials Letters, 2012, 72, 25-28.	2.6	33
74	Axial p–n Nanowire Gated Diodes as a Direct Probe of Surface-Dominated Charge Dynamics in Semiconductor Nanomaterials. Journal of Physical Chemistry C, 2011, 115, 23552-23557.	3.1	9
75	Electrochemical growth of vertically aligned ZnO nanorod arrays on oxidized bi-layer graphene electrode. CrystEngComm, 2011, 13, 6036.	2.6	30
76	Aluminum Nanotransmission Lines with No Grain Boundaries and No Surface Roughness. Applied Physics Express, 2011, 4, 064104.	2.4	1
77	RF Characterization of Germanium Nanowire Field Effect Transistors. AIP Conference Proceedings, 2011, , .	0.4	0
78	Catalyst-free growth of Sb2Te3 nanowires. Materials Letters, 2011, 65, 812-814.	2.6	6
79	Drastic improvement of oxide thermoelectric performance using thermal and plasma treatments of the InGaZnO thin films grown by sputtering. Acta Materialia, 2011, 59, 6743-6750.	7.9	66
80	Analytical Characteristics of Electrochemical Biosensor Using Ptâ€Đispersed Graphene on Boron Doped Diamond Electrode. Electroanalysis, 2011, 23, 2408-2414.	2.9	20
81	Electrical characteristics of nickel silicide–silicon heterojunction in suspended silicon nanowires. Solid-State Electronics, 2011, 56, 130-134.	1.4	8
82	Organic Electrolyte Based Pulsed Nanoplating and Fabrication of Carbon Nanotube Network Transistors. Japanese Journal of Applied Physics, 2011, 50, 06GE11.	1.5	1
83	Graphene arch gate SiO2 shell silicon nanowire core field effect transistors. Applied Physics Letters, 2011, 99, 212102.	3.3	5
84	Large-Scale Solution-Phase Growth of Cu-Doped ZnO Nanowire Networks. Journal of Nanoscience and Nanotechnology, 2011, 11, 6062-6066.	0.9	2
85	Organic Electrolyte Based Pulsed Nanoplating and Fabrication of Carbon Nanotube Network Transistors. Japanese Journal of Applied Physics, 2011, 50, 06GE11.	1.5	13
86	Deoxyribonucleic Acid Sensitive Graphene Field-Effect Transistors. IEICE Transactions on Electronics, 2011, E94-C, 826-829.	0.6	0
87	Synthesis of Small Diameter Silicon Nanowires on SiO2 and Si3N4 Surfaces. IEICE Transactions on Electronics, 2010, E93-C, 546-551.	0.6	1
88	Pt-polyaniline nanocomposite on boron-doped diamond electrode for amperometic biosensor with low detection limit. Mikrochimica Acta, 2010, 171, 249-255.	5.0	36
89	Amperometric hydrogen peroxide biosensor based on a modified gold electrode with silver nanowires. Journal of Applied Electrochemistry, 2010, 40, 2099-2105.	2.9	76
90	P-type silicon nanowire-based nano-floating gate memory with Au nanoparticles embedded in Al2O3 gate layers. Solid State Sciences, 2010, 12, 745-749.	3.2	5

#	Article	IF	CITATIONS
91	Stretchable, Transparent Zinc Oxide Thin Film Transistors. Advanced Functional Materials, 2010, 20, 3577-3582.	14.9	133
92	Fabrication of vertically aligned Si nanowires on Si (100) substrates utilizing metal-assisted etching. Journal of Vacuum Science and Technology A: Vacuum, Surfaces and Films, 2010, 28, 735-740.	2.1	11
93	Microwave Characterization of a Field Effect Transistor with Dielectrophoretically-Aligned Single Silicon Nanowire. Japanese Journal of Applied Physics, 2010, 49, 06GG12.	1.5	9
94	Non-enzymatic electrochemical CuO nanoflowers sensor for hydrogen peroxide detection. Talanta, 2010, 80, 1648-1652.	5.5	280
95	Fabrication of graphene field-effect transistors by simple stripping from CVD-grown layers. , 2010, , .		1
96	Catalyst-free Growth of Single-Crystal Silicon and Germanium Nanowires. Nano Letters, 2009, 9, 864-869.	9.1	88
97	pH dependent electrical characteristic of bottom-up synthesized silicon nanowire FETs with DDT passivation. , 2009, , .		0
98	Extracting Mobility Degradation and Total Series Resistance of Cylindrical Gate-All-Around Silicon Nanowire Field-Effect Transistors. IEEE Electron Device Letters, 2009, 30, 665-667.	3.9	10
99	Template-Assisted CVD Growth of Silicon Nanowires on a Gram Scale. Journal of the Korean Physical Society, 2009, 54, 152-156.	0.7	5
100	Amperometric Glucose Biosensor Based on a Pt-Dispersed Hierarchically Porous Electrode. Journal of the Korean Physical Society, 2009, 54, 1612-1618.	0.7	8
101	Electrical characteristics of Si-nanoparticle/Si-nanowire-based field-effect transistors. Journal of Materials Science, 2008, 43, 3424-3428.	3.7	5
102	Electrical characteristics of the back-gated bottom-up silicon nanowire field effect transistor. , 2008, , .		0
103	Fabrication of one-dimensional devices by a combination of AC dielectrophoresis and electrochemical deposition. Nanotechnology, 2008, 19, 105305.	2.6	16
104	Fabrication and Characterization of Sidewall Defined Silicon-on-Insulator Single-Electron Transistor. IEEE Nanotechnology Magazine, 2008, 7, 544-550.	2.0	5
105	Microwave Characterization of a Single Wall Carbon Nanotube Bundle. Japanese Journal of Applied Physics, 2008, 47, 4965-4968.	1.5	15
106	GROWTH OF HIGH QUALITY ZINC OXIDE NANOWIRES BY SIMPLE OXIDATION OF ZINC POWDER IN AIR. Nano, 2008, 03, 477-482.	1.0	2
107	Electrical Characteristics of the Backgated Bottom-Up Silicon Nanowire FETs. IEEE Nanotechnology Magazine, 2008, 7, 683-687.	2.0	10
108	Large-Scale Hierarchical Organization of Nanowires for Functional Nanosystems. Japanese Journal of Applied Physics, 2004, 43, 4465-4470.	1.5	65

#	Article	IF	CITATIONS
109	Scalable Interconnection and Integration of Nanowire Devices without Registration. Nano Letters, 2004, 4, 915-919.	9.1	337
110	Large-Scale Hierarchical Organization of Nanowire Arrays for Integrated Nanosystems. Nano Letters, 2003, 3, 1255-1259.	9.1	813
111	Nanolithography Using Hierarchically Assembled Nanowire Masks. Nano Letters, 2003, 3, 951-954.	9.1	151
112	Designed Self-Assembly of Molecular Necklaces. Journal of the American Chemical Society, 2002, 124, 2140-2147.	13.7	201
113	Transition Metal Ion Directed Supramolecular Assembly of One- and Two-Dimensional Polyrotaxanes Incorporating Cucurbituril. Chemistry - A European Journal, 2002, 8, 498-508.	3.3	166
114	A Two-Dimensional Polyrotaxane with Large Cavities and Channels: A Novel Approach to Metal-Organic Open-Frameworks by Using Supramolecular Building Blocks. Angewandte Chemie - International Edition, 2001, 40, 399-402.	13.8	195
115	Columnar one-dimensional coordination polymer formed with a metal ion and a host–guest complex as building blocks: potassium ion complexed cucurbituril. Inorganica Chimica Acta, 2000, 297, 307-312.	2.4	102
116	A homochiral metal–organic porous material for enantioselective separation and catalysis. Nature, 2000, 404, 982-986.	27.8	3,805
117	Self-Assembly of Interlocked Structures and Open Framework Materials using Coordination Bonds. Molecular Crystals and Liquid Crystals, 2000, 342, 29-38.	0.3	16
118	Self-Assembly of Interlocked Structures: Rotaxanes, Polyrotaxanes and Molecular Necklaces. Molecular Crystals and Liquid Crystals, 1999, 327, 65-70.	0.3	21
119	Shape-Induced, Hexagonal, Open Frameworks: Rubidium Ion Complexed Cucurbituril. Angewandte Chemie - International Edition, 1999, 38, 641-643.	13.8	146
120	A Molecular Bowl with Metal Ion as Bottom: Reversible Inclusion of Organic Molecules in Cesium Ion Complexed Cucurbituril. Angewandte Chemie - International Edition, 1998, 37, 78-80.	13.8	204
121	Molecular Necklace:Â Quantitative Self-Assembly of a Cyclic Oligorotaxane from Nine Molecules. Journal of the American Chemical Society, 1998, 120, 4899-4900.	13.7	213
122	Helical polyrotaxane: cucurbituril â€~beads' threaded onto a helical one-dimensional coordination polymer. Chemical Communications, 1997, , 2361-2362.	4.1	117
123	Polycatenated Two-Dimensional Polyrotaxane Net. Journal of the American Chemical Society, 1997, 119, 451-452.	13.7	291
124	Self-Assembly of a Polyrotaxane Containing a Cyclic "Bead―in Every Structural Unit in the Solid State:Â Cucurbituril Molecules Threaded on a One-Dimensional Coordination Polymer. Journal of the American Chemical Society, 1996, 118, 11333-11334.	13.7	228
125	Molecular Container Assembly Capable of Controlling Binding and Release of Its Guest Molecules:Â Reversible Encapsulation of Organic Molecules in Sodium Ion Complexed Cucurbituril. Journal of the American Chemical Society, 1996, 118, 9790-9791.	13.7	342
126	A Simple Construction of a Rotaxane and Pseudorotaxane: Syntheses and X-Ray Crystal Structures of Cucurbituril Threaded on Substituted Spermine. Chemistry Letters, 1996, 25, 503-504.	1.3	64

#	Article	IF	CITATIONS
127	The chemistry and catalytic activity of new cationic ruthenium(II) complexes in the hydrogenation of cyclohexene. Crystal structure of [RuH(CO)(PPh3)(P(OMe)3)(Ph2PCH2CH2AsPh2)]ClO4A·nâ^C5H12. Polyhedron, 1996, 15, 1473-1479.	2.2	4
128	Homogeneous hydrogenation with new cationic ruthenium(II) complexes of [RuH(CO)(NCCH3)(PPh3)2(diphos)]+ and [RuH(CO)(NCCH3)(PPh3)(diphos)]+. Crystal structure of [RuH(CO)(NCCH3)(PPh3) (Fe(η5-C5H4PPh2)2)][BF4]. Polyhedron, 1996, 15, 3811-3820.	2.2	8
129	Crystal structures of (±)-1,4-di-O-benzoyl-2,3-O-isopropylidene-myo-inositol and (±)-1,4-di-O-benzoyl-5,6-O-isopropylidene-myo-inositol: a conformational analysis. Carbohydrate Research, 1996, 295, 1-6.	2.3	0
130	Synthesis and characterization of a di-N-hydroxyethylated tetraaza macrocycle and its nickel(II) and copper(II) complexes: crystal structure of the nickel(II) complex. Journal of the Chemical Society Dalton Transactions, 1995, , 363.	1.1	45
131	Crystal structures of (±)-1,2:4,5-di-O-isopropylidene-myoinositol and (±)-1,2:5,6-di-O-isopropylidene-myo-inositol: a conformational analysis. Carbohydrate Research, 1994, 253, 13-18.	2.3	18
132	The catalytic activity of new ruthenium(II) complexes containing chelating diphosphine ligand in the homogeneous hydrogenation of cyclohexene. Polyhedron, 1994, 13, 1887-1894.	2.2	15
133	Two new [Cd(CN)2]nframeworks with linear channels of large, elongated hexagonal cross-section: structures of cadmium cyanide–guest (guest = dmf and Me2SO) clathrates. Journal of the Chemical Society Chemical Communications, 1994, , 637-638.	2.0	16
134	Synthesis, characterization and structure of the highly sterically congested complex (3,14-dimethyl-14-nitromethyl-2,6,13,17-tetraazatricyclo[16.4.0.07.12]docos-2-ene)nickel diperchlorate and structure of (3,14-dimethyl-2,6,13,17-tetraazatricyclo[16.4.0.07.12]docosa-2,13-diene)nickel diperchlorate. Journal of the Chemical Society Dalton Transactions, 1994, , 853.	1.1	9
135	Aromatic-aromatic ring interactions tested in cyclophanes. Bioorganic and Medicinal Chemistry Letters, 1993, 3, 263-268.	2.2	17
136	Guest-dependent [Cd(CN)2]nhost structures of cadmium cyanide–alcohol clathrates: two new [Cd(CN)2]nframeworks formed with PrnOH and PriOH guests. Journal of the Chemical Society Chemical Communications, 1993, , 1400-1402.	2.0	41
137	Synthesis, characterization and crystal structures of novel hafnium porphyrins. Journal of the Chemical Society Dalton Transactions, 1993, , 205.	1.1	22
138	Asymmetric induction in silyl nitronate cycloadditions to Oppolzer's chiral sultam derivatives. Tetrahedron: Asymmetry, 1991, 2, 27-30.	1.8	32